

# Enhancement of solar cell efficiency by using TiO<sub>2</sub> nanostructure doped Fe<sub>2</sub>O<sub>3</sub> dye and effect concentration of solvent on optical properties

## ABSTRACT

Solar energy has the greatest potential of all the sources of renewable energy, as only a small amount of this form of energy could be used, especially when other sources (coal, oil or gas) in the country have depleted. A solar cell is a solid electrical device that converts solar energy directly to electricity. Hybrid solar cells based on inorganic and organic compounds are a promising renewable energy source.

**Aims:** The aim of this study was to prepare a nanostructure thin film of titanium oxide: doped iron oxide for enhancement of the solar cell efficiency. In addition to study the effect doped on optical properties of titanium oxide nanostructure thin film.

**Study design :** The spray pyrolysis deposition method used for preparation the nanostructure material

**Place and Duration of Study:** This study was conducted in department of physics and department of materials sciences, Al-neelain university, between January 2016 and January 2019.

**Methodology:** Thin films of Titanium Oxide (TiO<sub>2</sub>) doped Iron Oxide (Fe<sub>2</sub>O<sub>3</sub>) have been prepared by chemical spray pyrolysis deposition technique. A laboratory designed glass atomizer was used for spraying the aqueous solution. Which has an output nozzle about 1mm. then film were deposited on preheated cleaned glass substrates at temperature of 400 °C. we used different concentration to study optical parameters. A 1.5 g TiO<sub>2</sub> powder of anatase structure doped with 1.5 g of Fe<sub>2</sub>O<sub>3</sub> was mixed with 2 ml of ethanol and stirred using a magnetic stirrer for 30 minutes to form TiO<sub>2</sub> paste to obtain the starting solution for deposition and spray time was 10 s and spray interval 2 min was kept constant. The carrier gas (filtered compressed air) was maintained at a pressure of 10<sup>5</sup> Nm<sup>-2</sup>, and distance between nozzle and substrate was about 30 cm ± 1 cm. Thickness of sample was measured using the weighting method and was found to be around 400 nm. Optical transmittance and absorbance were record in wavelength range of (200-1100) nm using UV-Visible spectrophotometer (Shimadzu Company Japan).

**Results:** The results obtained showed that the optical band gap decreased from 5.58 eV before doping to (3.9, 3.81, 3.81 and 3.81 eV) after doped for TiO<sub>2</sub>:Fe<sub>2</sub>O<sub>3</sub> thin films, this result refer to the broadening of secondary levels that product by TiO<sub>2</sub>: doping to the Fe<sub>2</sub>O<sub>3</sub> thin films. Also the results showed the variation of refractive index with wavelength for different concentration after doped of TiO<sub>2</sub>:Fe<sub>2</sub>O<sub>3</sub> films from this figure, it is clear that n decrease with low concentration and increase with high concentration after doped that mean the density is decreased of this films. In addition the extinction coefficient of TiO<sub>2</sub>:Fe<sub>2</sub>O<sub>3</sub> thin films recorded before doped and with different concentration (1.1, 1.2, 1.5 and 1.6 mol/L) and in the range of (300 – 1200) nm and after doped it observed from that the extinction coefficient, decrease sharply with the increase of wavelength for all prepared films and all the sample after doped is interference between them accept the sample before annealing is far from the other sample.

**Conclusion:** Based on the results obtained doping of titanium oxide increase the efficiency of TiO<sub>2</sub> thin film in DSSC. It also proves that the fabrication of TiO<sub>2</sub> thin films by spray pyrolysis deposition method is successful.

**Keywords:** solar energy, photovoltaic, Nanostructure, dye-sensitized

# 1. INTRODUCTION

In the modern world of technological advancements, energy has become one of the basic needs for life. With the increase in world population, so is rising the energy demand. The worldwide power consumption is expected to double in the next 3 decades, and the limited supply of fossil fuels is hardly expected to cope with this. Nuclear power, though capable of providing large scale power generation, is being proven to be guilty in safety and waste management issues. Hence, sooner or later we need to turn to renewable energy sources, and the most viable candidate of them is solar energy [1]. A solar cell is a solid electrical device that converts solar energy directly to electricity. There are two fundamental functions of solar cells: photo-generation of charge carriers (electrons and holes) in a light-absorbing material and separation of the charge carriers to a conductive interaction to transmit electricity. Adding to the wide range of solar cells, hybrid solar cells based on inorganic and organic compounds are a promising renewable energy source. Solar cells are one type of photovoltaic cells which generate electrical power by converting energy of light into direct current electricity by using semiconductors that exhibit the photovoltaic effect. In the photovoltaic effect, electrons are transferred between different bands (usually from the valence bands to conduction bands) within the material, resulting in the buildup of voltage between two electrodes. **The first step in solar cell always involves photon absorption by a semiconducting material. When the photon is absorbed, the energy of photon will be transferred to valence electrons, which excite an electron to another band, called the conduction band, in which, electrons can freely move [2].** Photovoltaic devices are the primary solar energy conversion systems to harvest the solar energy. These photovoltaic devices, more simply known as solar cells, convert the incident photon energy of the solar radiation into electrical energy through the generation and subsequent collection of electron-hole pairs. There are several challenges that need to be met for the solar cell technologies to make it a pragmatic solution to our energy crisis. Photovoltaic devices based on nanostructure materials cells have been previously proposed due to their potential to provide high-energy conversion efficiency [2]. The large energy conversion efficiency arises from the following effects, nanostructure crystallite sizes are comparable to the carrier scattering lengths, this significantly reduces the scattering rate, thus increasing the carrier collection efficiency, nanostructures have strong absorption coefficient due to increased density of states. In addition, by varying the size of the nanostructures, the band gap can be tuned to absorb in a particular photon energy range and size-dependent properties of nanostructures such as quantum size effects in semiconductor nanoparticles provide the basis for developing newer and effective systems [3]. With the development of metal oxide-based solar cells, or so called dye-sensitized solar cells (DSSC), conventional solid state photovoltaic technologies are now challenged by devices functioning at a molecular and nanometer level. The important means of producing high-efficiency solar cells are reducing reflectance, trapping light in the cell and increasing light absorption [4]. Silicon solar cells have achieved electricity conversion efficiencies ranging from 15% to 20% [5]. However, the high fabrication cost and the usage of toxic chemicals in producing highly purified silicon during the manufacturing process has motivated the search for an environmentally friendly, low-cost solar cell. Dye-sensitized solar cells (DSSC) have received considerable attention since O'Regan and Grätzel reported a remarkably high conversion efficiency of nearly 10% [6]. Using Nano crystalline mesoporous TiO<sub>2</sub> film. However, these organic solar cells are still limited to low power conversion efficiencies [7]. The prospects of low-cost initial investments, cheap component materials without the need for expensive doping and purification, and relatively simple production technologies are quite attractive. One particular advantage of DSSC in comparison with other competing technologies is their ability to perform relatively better under diffuse light conditions and elevated temperatures [8]. **DSSC** are photonic devices that convert visible light into electricity and are based on a porous thin film of a wide-band gap semiconductor oxide modified by dye molecules. The manufacturing cost of DSSC, which are 3rd-generation solar cells, is approximately 1/3 to 1/5 times that of silicon solar cells [8]. Amongst these various solar cells, there is a boost in dye-sensitized solar cells which provide a technically and economically credible alternative concept to present day p-n junction photovoltaic devices. DSSC captured the attention of the international research community in 1991 with the report of a 7% efficient cell by O'Regan and Grätzel. The efficiency of DSSC has increased considerably in last 20 years, with the confirmed record now standing at 11% [9]. This type of film enhances the light absorption due to its sponge-like characteristics and increased surface area. The Nano-crystalline material plays an essential role in electron injection and transport, determining the performance of the **DSSC** [9]. The overall conversion efficiency of DSSC was reported to be proportional to the injection of electrons in wide-band gap nanostructured semiconductors. To date, the certified efficiency record is approximately 11.1% for a small cell, and large-scale tests have clarified the great need for the commercialization of **DSSC** [10]. Thus, **DSSC**

have numerous advantages over silicon solar cells. DSSC is the only solar cell that separates the two functions of light harvesting and charge carrier transport. All other conventional and OPV technologies perform both operations simultaneously. This separation opens up a vast amount of options for engineering and optimizing the different parts and functions of the cell individually [11]. Generally, DSSC are mainly composed of three parts: the dye-sensitized semiconductor Nano crystalline film photo anode, the redox couple (usually I<sup>3</sup>/I<sup>-</sup>) in organic solvent(s), and the platinized transparent conducting oxide (TCO) glass as the counter electrode. Among those, the photo anode consists of porous semiconductor Nano crystalline film adsorbed by dye molecules (such as a ruthenium complex), which can absorb the light energy especially the visible light of sunshine [12]. The dye molecules move to the excited states when the DSSC is exposed to light irradiation with suitable energy, and the excited state electrons are injected quickly into the conduction band of semiconductor; these injected electrons are collected through the conducting substrate of the photo anode. [13]. Unlike the crystalline and thin film solar cells that have solid-state light absorbing layers, dye sensitized solar cells is composed of a dye adsorbed semiconductor (TiO<sub>2</sub>, ZnO, SnO<sub>2</sub>, etc.) electrode, a liquid electrolyte containing the redox couple I<sup>-</sup>/I<sup>3</sup>- sandwiched between glasses having transparent conductive oxide layer. The DSSC consist of sensitizing dye, nanoparticles, and electrolyte. The mechanism of the dye sensitized solar cell has three steps, a dye, adsorbed on a layer of semiconductor interacts with the visible light provided by the sun (just like the green pigment does in a leaf), promoting an electron from a lower level orbital to an excited one. Photo-excitation occurs when the photons from the light source penetrate the solar cell to excite the dye's electrons, the excited electron is injected by the dye into the semiconductor and, the chemical diffusion of electrons from the semiconductor layer into the FTO/ITO conductive layer occurs when the multi meter is connected creating the outside circuit and the electrons return to the cell to complete the circuit and bring the dye back to its "normal" DSSC proposed by O'Regan and Grätzel has attracted substantial interest since 1991, due to its characteristics, such as low production cost, and low environmental impact during fabrication state by using an electrolyte solution that helps carry electrons through the cell [13]. The need for DSSC to absorb far more of the incident light was the driving force for the development of mesoscopic semiconductor materials with an enormous internal surface area. Various semiconductors such as TiO<sub>2</sub> [14], BaTiO<sub>3</sub> [15], SnO<sub>2</sub> [16], ZnO [17], Nb<sub>2</sub>O<sub>5</sub> [18], and Zn<sub>2</sub>SnO<sub>4</sub> [19] have been used as an anode material, are relatively wide band gap materials and generally transparent to visible light. Narrow band gap materials such as GaAs, Fe<sub>2</sub>O<sub>3</sub> and CdS get easily corroded in contact with the electrolyte. Among these anode materials ZnO and TiO<sub>2</sub> having wide band gap are suitable materials for DSSC due to their excellent electrochemical stability [20]. TiO<sub>2</sub> is a semiconductor having three polymorphisms including tetragonal rutile, tetragonal, anatase and orthorhombic brookite. Rutile structure is the most thermodynamically stable phase, while the other two are metastable. TiO<sub>2</sub> of anatase phase has wider energy band gap of 3.2eV compared to the rutile phase which has 3.0eV, and hence it has better photo-activity performance and suitable for DSSC application [21]. Besides semiconductor material, dye also plays an important role in enhancing DSSC performance since it should be able to harvest the sunlight and transfer it into electrical energy. Many researches have been conducted on **DSSC** using different types of dyes including natural and synthetic dyes. The main characteristic of the dye is its ability in absorbing the visible light spectrum from red to blue so that it can sensitize the wide band gap semiconductor material [22]. The Dye Sensitized Solar Cell (DSSC) uses the same basic principle as plant photosynthesis to generate electricity from sunlight. Each plant leaf is a photo-chemical cell that converts solar energy into biological material. Although only 0.02-0.05% of the incident solar energy is converted by the photosynthesis process, the food being produced is 100 times more than what is needed for mankind.15the chlorophyll in green leaves generate electrons using the photon energy, which triggers the subsequent reactions to complete the photosynthesis process [23]. Dye-sensitized solar cells operate differently from other types of solar cells in many ways with some remarkable analogies to the natural process of photosynthesis. Therefore, this system has repeatedly been described in terms of artificial photosynthesis since the interest in **DSSC** took off with the landmark publication by O'Regan and Gratzel in the early 1990's Like the chlorophyll in plants, a monolayer of dye molecules (sensitizers) absorbs the incident light, giving rise to the generation of positive and negative charge carriers. A typical DSSC consists of a transparent conductive oxide (TCO), semiconductor oxide, desensitizer, electrolyte and counter electrode. The working electrode is a Nano porous semiconductor oxide that is placed on conducting glass and is separated from the counter electrode by only a thin layer of electrolyte solution.. The extension of the photo electrode dye enables the collection of lower energy photons [24]. The dye is chemisorbed onto the semiconductor oxide surface. An ideal sensitizer should adsorb a wide range of wavelengths and possess high thermal stability due to its strong binding to the semiconductor oxide. The photo anode of DSSCs is typically constructed using a thick film (~10µm) of TiO<sub>2</sub> or, less often, ZnO or SnO<sub>2</sub> nanoparticles [25].

The TiO<sub>2</sub> film has a large inherent absorptive surface area for light scattering. One challenge in the fabrication of DSSCs involves the matching of the material band gaps and the structure design for each layer to give the maximum photoelectrochemical output and thereby the maximum conversion efficiency. The aim of this study was to prepare a nanostructure thin film of titanium oxide: doped iron oxide for enhancement of the solar cell efficiency. In addition to study the effect doped on optical properties of titanium oxide nanostructure thin film.

## 2. MATERIAL AND METHODS

### 2.1 Preparation of the TiO<sub>2</sub>: Fe<sub>2</sub>O<sub>3</sub> films by chemical spray pyrolysis deposition technique

TiO<sub>2</sub> thin film prepared by spray pyrolysis deposition (SPD) method which involves spraying the solution onto substrate placed over a heated surface where the solvent will evaporate to form a solid chemical compound. The compound used to produce a thin film by this method should be volatile at the temperature of deposition. Thin films of Titanium Oxide (TiO<sub>2</sub>) doped Iron Oxide (Fe<sub>2</sub>O<sub>3</sub>) have been prepared by chemical spray pyrolysis deposition technique. Iron oxide ( $\alpha$ -Fe<sub>2</sub>O<sub>3</sub>) is used as a dye at different concentration. 1.5 mg of Fe<sub>2</sub>O<sub>3</sub> is dissolved in 2mL of Ethanol. The dye solution is stirred at room temperature for 30 minutes in magnetic stirrer. The TiO<sub>2</sub> coated FTO substrates were soaked in the dye solution for 15 min. The dye sensitized electrode in different concentration was prepared for all the samples by this method. A laboratory designed glass atomizer was used for spraying the aqueous solution. Which has an output nozzle about 1 mm. then film were deposited on preheated cleaned glass substrates at temperature of 400°C. we used different concentration to study optical parameters. A 1.5 mg TiO<sub>2</sub> powder structure doped with 1.5 mg of Fe<sub>2</sub>O<sub>3</sub> was mixed with 2 ml of ethanol and stirred using a magnetic stirrer for 30 minutes to form TiO<sub>2</sub> to obtain the starting solution for deposition and spray time was 10 s and spray interval 2 min was kept constant. The carrier gas (filtered compressed air) was maintained at a pressure of 105 Nm<sup>-2</sup>, and distance between nozzle and substrate was about 30 cm ± 1 cm. The spraying was done by making a left and right motion until all of the solution was deposited onto substrates. After the spraying process was done, the TiO<sub>2</sub> films that had been fabricated were put in the furnace for annealing process. The temperature was set at (450° and 500°). The period for annealing is 30 minute. Then, the samples were taken out from the furnace and let to cool down to room temperature before dipped into the dye.

### 2.3 DSSC Characterization:-

The XRD patterns were recorded on a Philips X'pert Pro MPD model X-ray diffract meter using Cu K $\alpha$  radiation as the X-ray source. The diffract grams were recorded in the 2 $\theta$  range of 10- 80°. The average crystallite size of TiO<sub>2</sub> phase was determined according to the Scherer equation. The morphology and size of Nano powders and films were characterized using scanning electron microscope (SEM) (JEOL JSM-7600F, Japan - 30JSM) equipped with an energy dispersive X-ray (EDS). The absorption spectra of dye solutions and dyes adsorbed on TiO<sub>2</sub> surface were recorded using a UV-VIS spectrophotometer (Shimadzu, model UV-4200).

#### 2.3.1 XRD characterization:-

Various structural parameters of the TiO<sub>2</sub> photo anode developed on ITO coated glass substrates at different annealing temperatures (450 °C, 500 °C) were investigated by X-ray diffract meter (GBC-EMMA, Australia) at 2 $\theta$  position (from 20° to 90°) with Cu K $\alpha$  X-ray of wavelength = 1.54056 Å.

#### 2.3.2 SEM characterization

SEM characterizations were carried out by FESEM (JEOL JSM-7600F, Japan) at 5 kV to 7 kV accelerating voltage.

#### 2.3.3 UV-Vis-Spectrophotometer

UV-Vis- spectra of TiO<sub>2</sub> films annealed at different temperatures were recorded by UV-Vis-NIR spectroscopy (Hitachi 4200, Japan).

### 3. RESULTS AND DISCUSSION

#### 3.1 Microstructure and morphological characteristic of the TiO<sub>2</sub> electrodes

The XRD patterns of TiO<sub>2</sub> NPs at different calcination temperatures are shown in Figure 1. The Nano crystalline structure was confirmed by (1 0 1), (0 0 4), (2 0 0), (1 0 5) and (2 1 1) diffraction peaks<sup>(31)</sup>. The XRD patterns of TiO<sub>2</sub> has a main peak at 2θ = 25.28 corresponding to the 101 planes (JCPDS 21-1272) while the main peaks of rutile and brookite phases are at 2θ = 27.48 (110 plane) and 2θ = 30.88 (1 2 1 plane). The prominent peaks representing anatase phase of nanocrystalline TiO<sub>2</sub> powder used for this study can be seen at the 2θ values of 25.28, 37. 80, 48.05, 53.89, 55.06, 62.69, 68.76, 70.31 and 75.03.

The (101) peak of TiO<sub>2</sub> becomes sharper and stronger with enhancing the annealing temperature from 500 to 700 °C. It is reasonable to speculate that the meso structures of TiO<sub>2</sub> NPs reconstructed along with the increase of crystallite size and crystallinity. Namely, the internal surface area of the TiO<sub>2</sub> film decreased with enhancing the annealing temperature, which is consistent with previous observation. This decrease in the internal surface area of TiO<sub>2</sub> film can also be confirmed by the decreasing absorbed amount of N719. The improvement in the crystallinity, decreases in the internal surface area, and the adsorbed amount of N719 will certainly affect the properties of DSSCs, which will be discussed further in the following section. Our observations indicate that the particles have relative high crystallinity, which is beneficial for the improvement of photo electrochemical properties of its corresponding film electrode. The amount of rutile in the samples was estimated using the Spurr equation [33]:-

$$FR = 1 \{1 + [0.8IA(101)/IR(110)]\} \dots\dots\dots (1)$$

Where FR is the mass fraction of rutile in the samples, IA(1 0 1) and IR(1 1 0) are integrated main peak intensities of anatase and rutile, respectively. Results shows the phase transformation from anatase to rutile starts in 600 0C. In addition to the anatase-to-rutile phase transformation, the average anatase crystallite size, as determined by applying the Scherrer equation to the anatase (101) peak, increased from 13 to 42 nm, about 70%, over the temperature range from 500 to 700 °C.

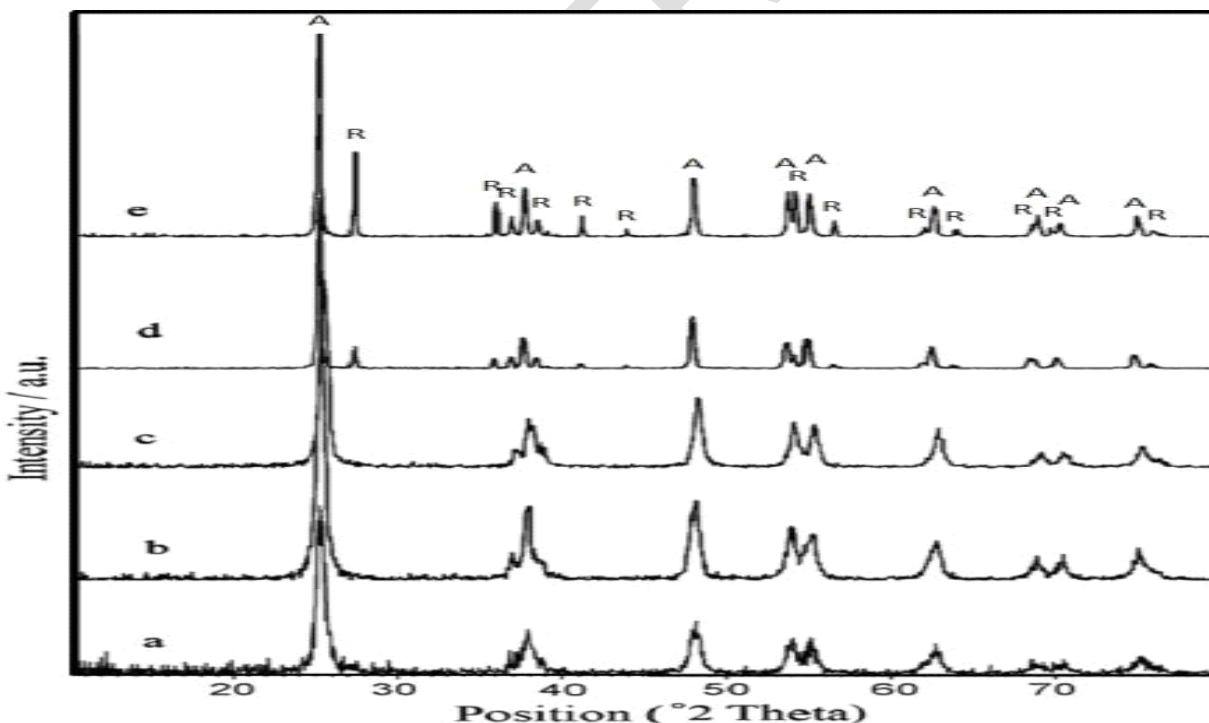
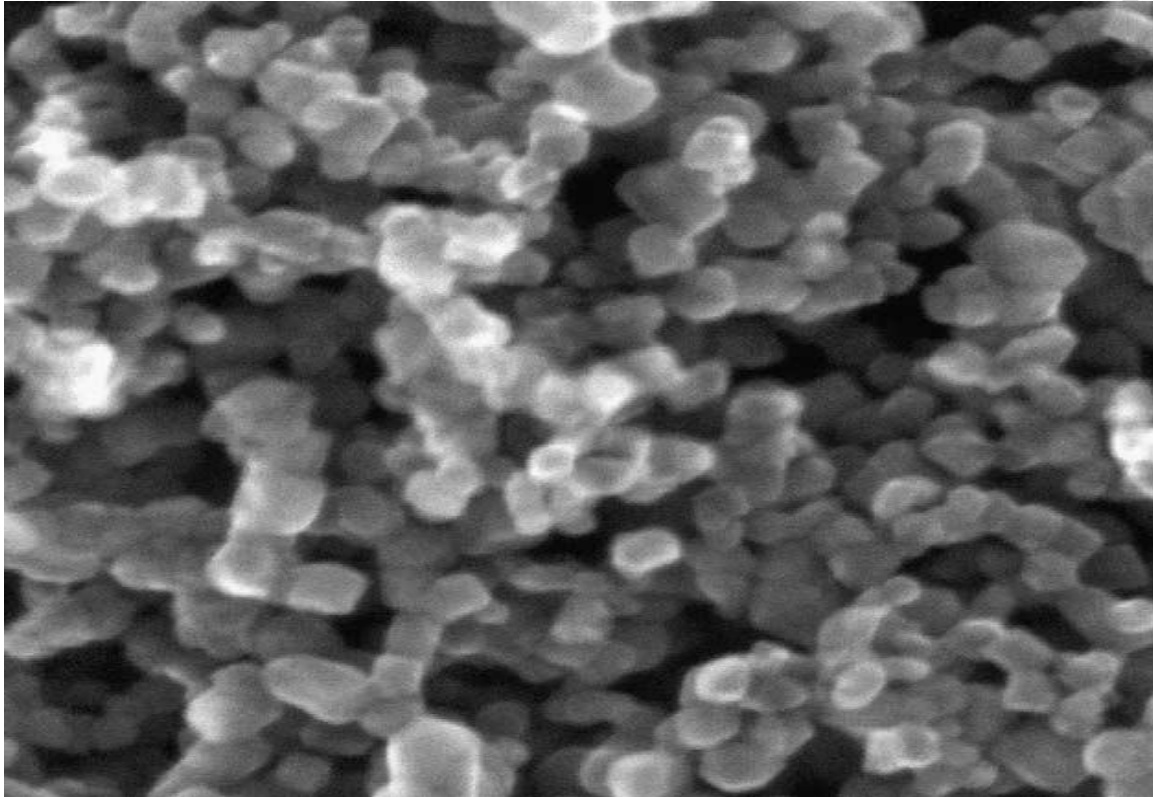


Fig.1. XRD patterns of TiO<sub>2</sub> nanoparticles before and after doped calcinated at different concentration (a) before, (b) 1.1mol/L, (c) 1.2mol/L, (d) 1.5mol/L, (e) 1.6mol/L (A).

Fig. 2 shows the scanning electron micrograph of a typical  $\text{TiO}_2$  film deposited by screen printing on a conducting glass sheet that serves as current collector. The film thickness is typically 5–20  $\mu\text{m}$  and the  $\text{TiO}_2$  mass about 1–4  $\text{mg}/\text{cm}^2$ . Analysis of the layer morphology shows the porosity to be about 50–65%, the average pore size being 15 nm. The prevailing structures of the anatase nanoparticles are square–bipyramidal, pseudo cubic and stablike. According to HRTEM measurements the (1 0 1) face is mostly exposed followed by (1 0 0) and (0 0 1) surface orientations. A recent alternative embodiment of the DSC concept is the sensitized hetero junction usually with an inorganic wide band gap Nano crystalline semiconductor of n-type polarity as electron acceptor, the charge neutrality on the dye being restored by a hole delivered by the complementary semiconductor, inorganic [4,5] or organic [6] and of p-type polarity. The prior photo-electrochemical variant, being further advanced in development, has an AM 1.5 solar conversion efficiency of over 10%, while that of the solid-state device is, as yet, significantly lower.



**Fig.2.** Scanning electron microscope picture of a nanocrystalline  $\text{TiO}_2$  film used in the dye-sensitized solar cell (DSSC)

Analysis of optical absorbance spectra (A), transmission (T) and reflectance (R) is one of the most productive tools for understanding the band structure and energy band gap ( $E_g$ ) of both amorphous and polycrystalline materials. To study effect of dopant on optical absorbance of  $\text{TiO}_2$ :  $\text{Fe}_2\text{O}_3$  thin films the dependence of absorbance on the wavelength ( $\lambda$ ) in the spectral range of (200 -1100) nm, was recorded. Fig (3), Fig (4) and Fig (5) are representing the relationship between the absorbance, transmittance and the Reflectance with wavelength respectively.

From Fig (3) represent absorbance spectra at concentration at (1.1, 1.2, 1.5 and 1.6) respectively it can notice that high value of absorbance spectra increase at concentration (1.6mol/L) and we found peak is very small sharp but found interference between absorbance spectra at concentration (1.2, and 1.6 mol/L) and all of absorbance spectra is start from 800nm and increase until 300nm.

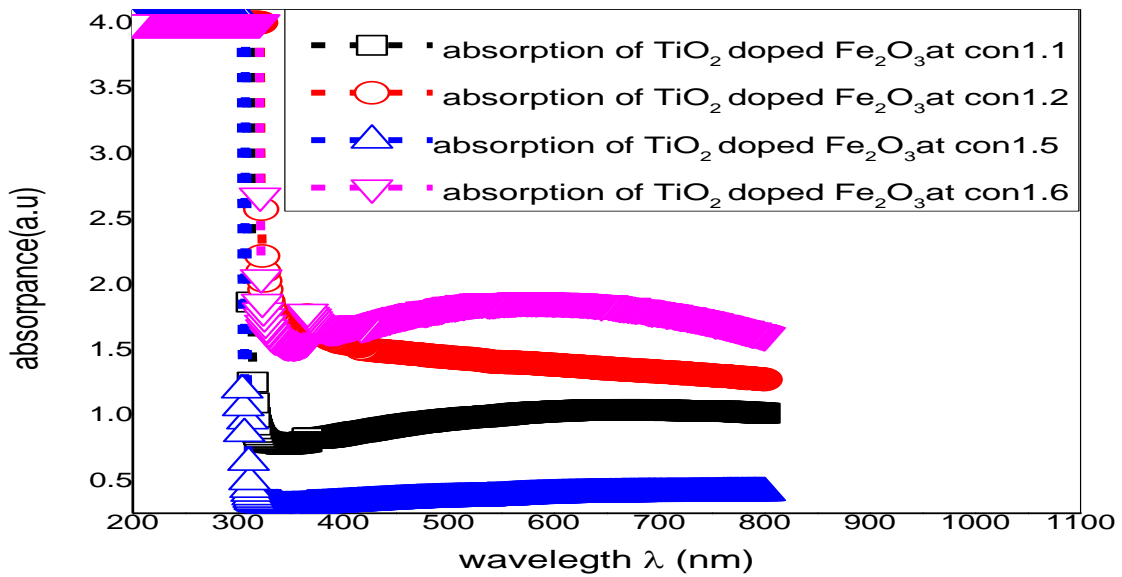


**Fig.(3). Absorption vs. wavelength plot of Fe<sub>2</sub>O<sub>3</sub>doped TiO<sub>2</sub> thin films at different concentration (1.1, 1.2, 1.5 and 1.6mol/L)**

From fig (4) it can be notice that the transmittance spectra at concentration 1.5mol/L represent high value but is shows that transmittance spectra increase with increase concentration and decrease with decrease concentration

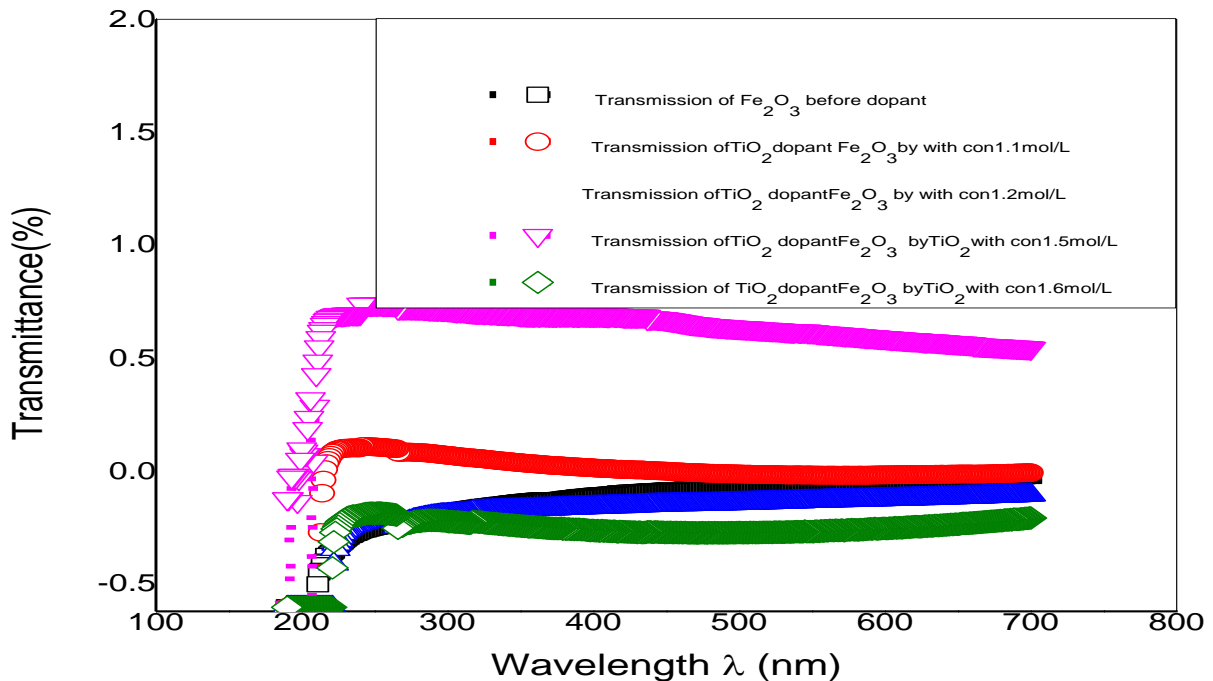


**Fig. (4).Transmission vs. wavelength plot of pure Fe<sub>2</sub>O<sub>3</sub> and after doped TiO<sub>2</sub> thin films at different concentration (1.1, 1.2, 1.5 and 1.6 mol/L)**

From fig (5) it can be notice that reflectance spectra decrease when concentration decrease but reflectance spectra with concentration (1.5mol/L) represent at low value but the reflectance is start increase from the wave length 300nm until to the wave length 350nm and return back another from wavelength from 360-400nm then become stable.

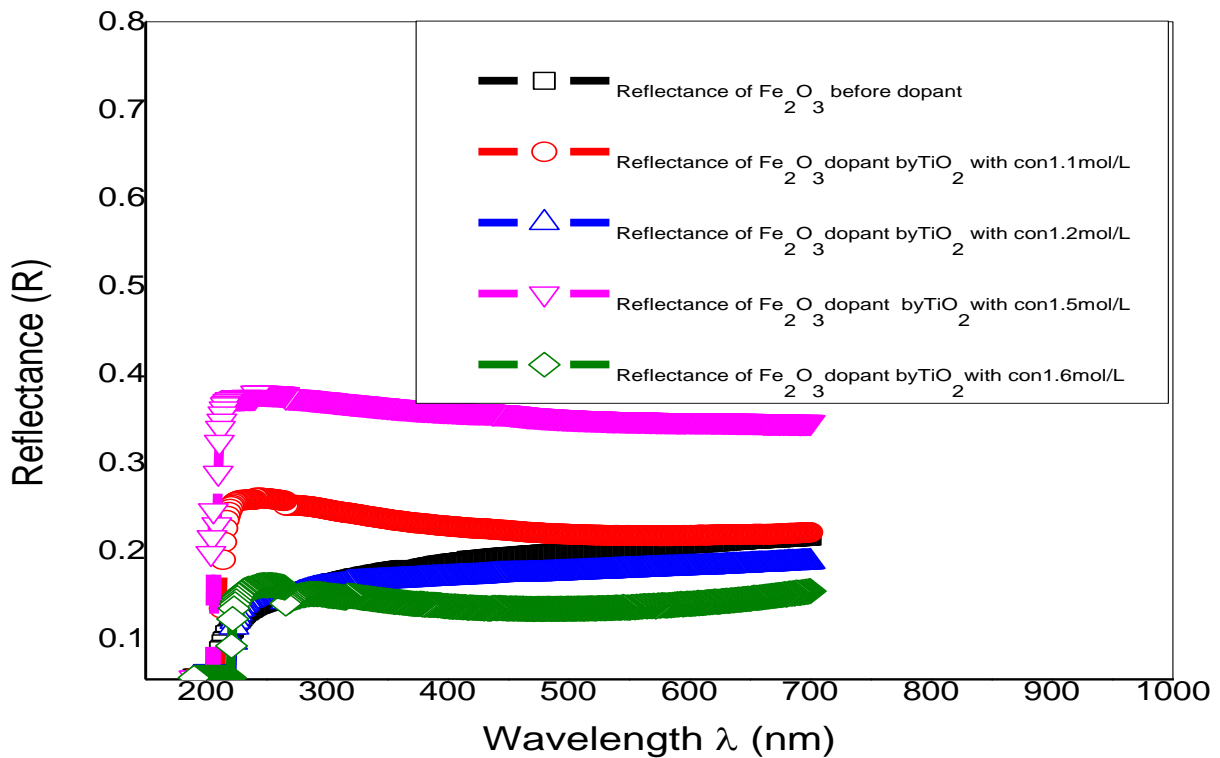


**Fig.(5). Reflectance vs. wavelength plot of Fe<sub>2</sub>O<sub>3</sub> before and after doped TiO<sub>2</sub> thin films at different concentration (1.1, 1.2, 1.5 and 1.6mol/L)**

The absorption coefficient  $\alpha(\lambda)$  of the doped TiO<sub>2</sub>: Fe<sub>2</sub>O<sub>3</sub> thin films can be calculated by simple method from transmittance spectra and defined as equation :-

$$T = \exp [-\alpha (\lambda) d] \tag{2}$$

Where T is the optical transmittance and d is the thickness of TiO<sub>2</sub>:Fe<sub>2</sub>O<sub>3</sub> thin films. A plot of absorption coefficient vs. wavelength is shown in fig (6). From this figure it can notice that the absorption coefficient is increase with gradually with photon energy until from 2.3 – 2.8 and 4eV. While the increases of  $\alpha$  become sharply and we show found interference at incident photon energy with concentration 1.6 and 1.2 equal 2.3eV but in case of before doped and with concentration 1.5 equal 4eV and with concentration 1.1 equal 2.8eV . In addition from this figure it can notice clearly the  $\alpha$  increases before doped and with high concentration after doped and high value of  $\alpha$  refer to the allowed direct transition for all prepared TiO<sub>2</sub>:FeO<sub>3</sub>.



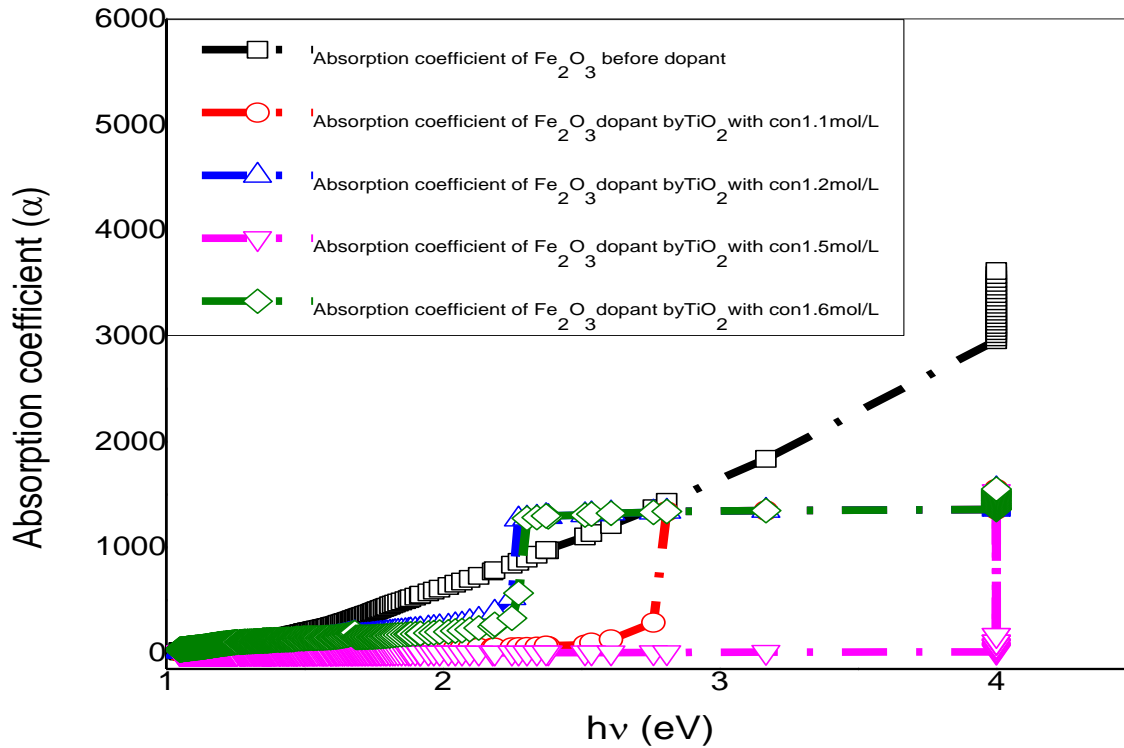


**Fig.(6). Absorption coefficient vs. wavelength plot of Fe<sub>2</sub>O<sub>3</sub> before doped and after doped TiO<sub>2</sub> thin films at different concentration (1.1, 1.2, 1.5 and 1.6 mol/L)**

There are many different methods for determining the optical band gap ( $E_g$ ). Yadav et al , Dghoughi et al, Pejova and coworkers , Ismail et al determined the band gap from the relation between the absorption coefficient ( $\alpha$ ) and the energy incident light

$$(\alpha h\nu)^n = B (h\nu - E_g) \tag{3}$$

Where  $h$  is the photon energy,  $B$  is constant, and  $n$  represents the transition type ( $n = 2$ ) for direct transition  $n = (1/2)$  for indirect transition). The values of direct optical band gap ( $E_g$ ) values of the TiO<sub>2</sub>:Fe<sub>2</sub>O<sub>3</sub> thin films were obtained from the intercept of  $(\alpha h)^2$  vs.  $h\nu$  curves plotted as shown in figs (7,8,9, 10 and 11 ) from these figures it can notice that the optical band gap decreased from 5.58eV before doped to ( 3.9eV , 3.81eV , 3.887eV and 3.818eV) after doped for TiO<sub>2</sub>:Fe<sub>2</sub>O<sub>3</sub> thin films, this result refer to the broadening of secondary levels that product by TiO<sub>2</sub>: doping to the Fe<sub>2</sub>O<sub>3</sub> thin films. The different between this figure from (7 – 11) the band gap is decreased from 5.58 before doped to (3.9eV , 3.81eV , 3.887eV and 3.818eV) after doped at different concentration ( 1.1, 1.2, 1.5, and 1.6 mol/L).

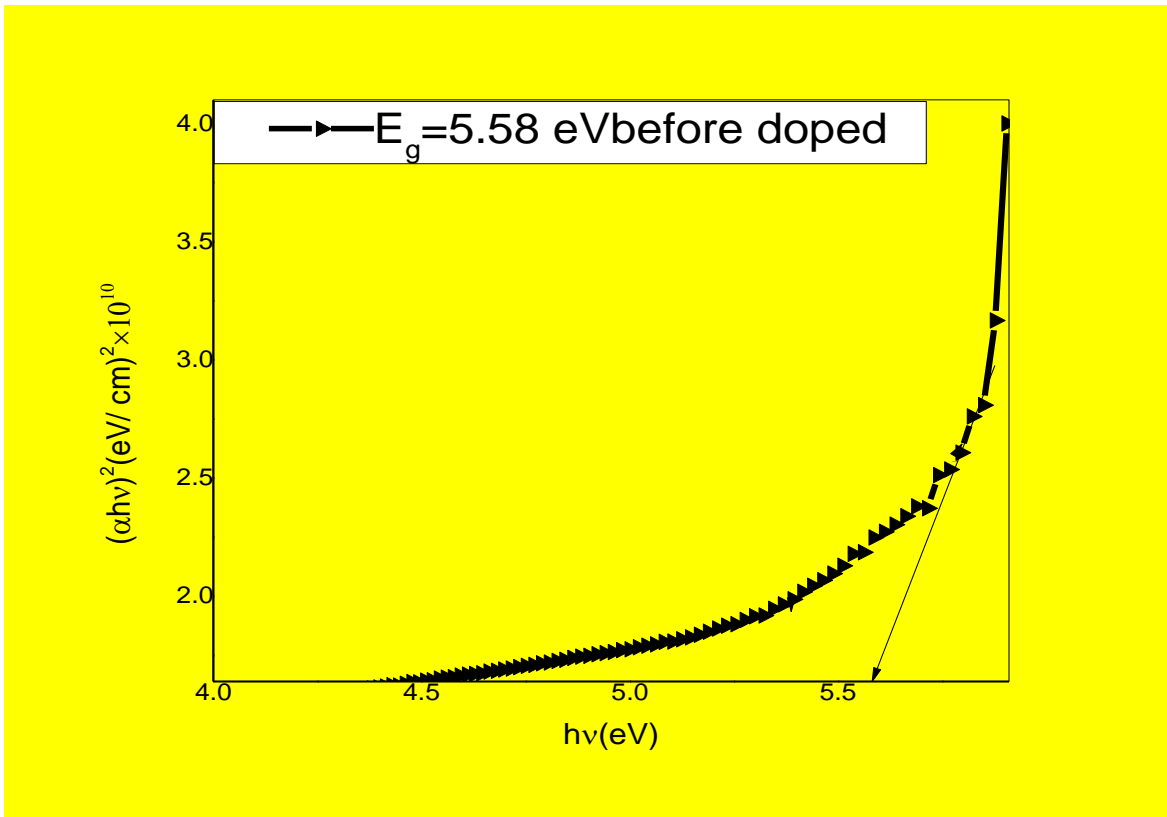


Fig. (7).  $(\alpha h\nu)^2$  vs  $(h\nu)$  plot of Fe<sub>2</sub>O<sub>3</sub> thin films before doped

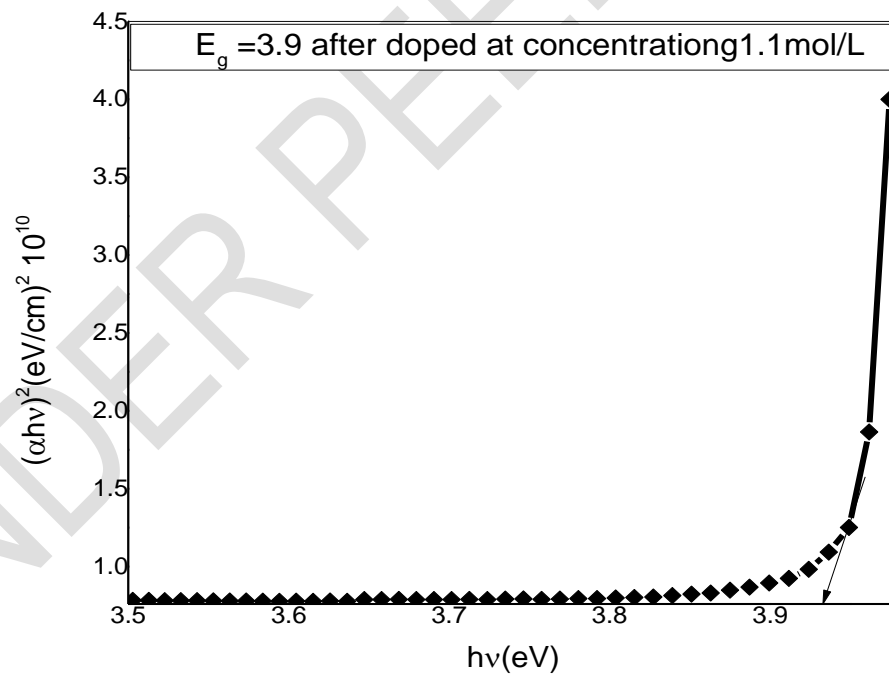


Fig. (8).  $(\alpha h\nu)^2$  vs  $(h\nu)$  plot of Fe<sub>2</sub>O<sub>3</sub> doped TiO<sub>2</sub> thin films with concentration 1.1 mol/L

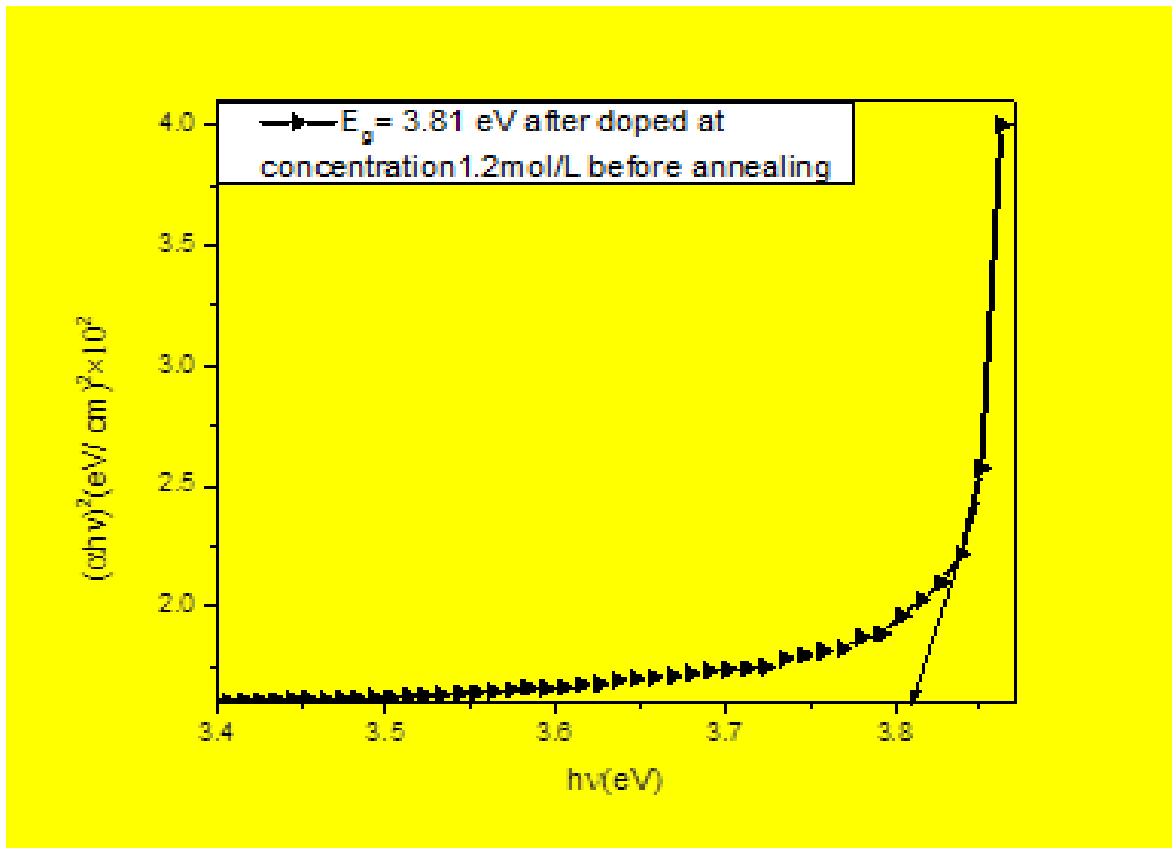


Fig (9)  $(\alpha h\nu)^2$  vs.  $(h\nu)$  plot of  $\text{Fe}_2\text{O}_3$  doped  $\text{TiO}_2$  thin films with concentration 1.2mol/L

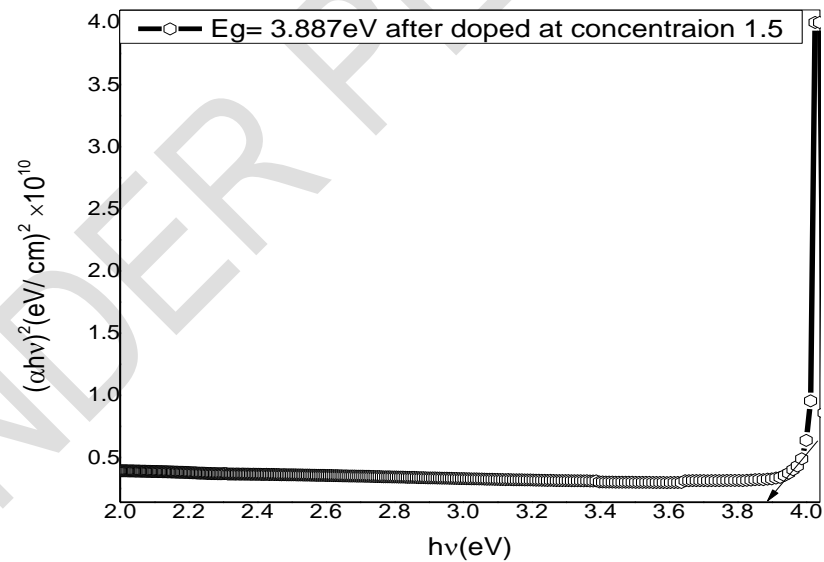


Fig (10)  $(\alpha h\nu)^2$  vs.  $(h\nu)$  plot of  $\text{Fe}_2\text{O}_3$  doped  $\text{TiO}_2$  thin films with concentration 1.5mol/L

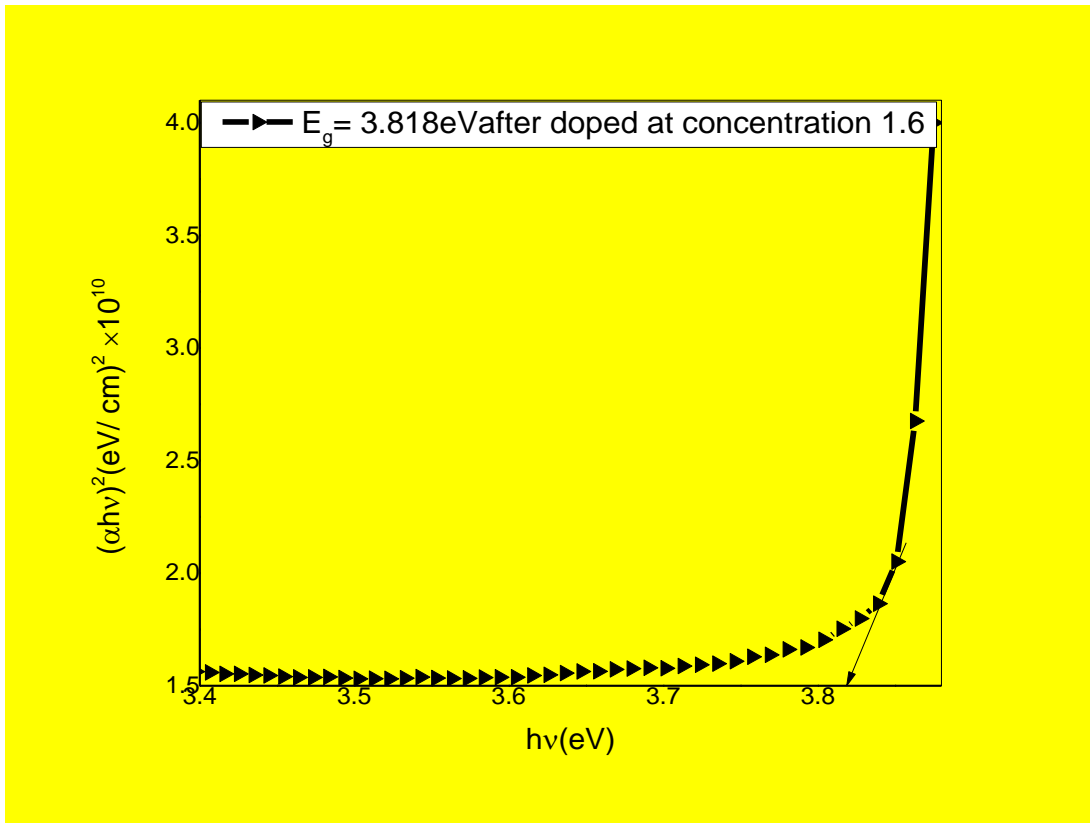


Fig. (11).  $(\alpha h\nu)^2$  vs.  $(h\nu)$  plot of  $\text{Fe}_2\text{O}_3$  doped  $\text{TiO}_2$  thin films with concentration 1.6mol/L

The refractive index dispersion plays an important role in the research of optical materials because it is a significant factor in optical communication and designing devices for spectral dispersion. The refractive index of the film was calculated Approximately from the following relation.

$$R = \frac{(n - 1)^2 - k^2}{(n + 1)^2 - k^2}$$

..... (4)

Where  $n$  is the refractive index and  $k$  is extinction coefficient. Fig (12) shows the variation of refractive index with wavelength for different concentration (1.1 – 1.2 – 1.5 – 1.6mol/L) after doped of  $\text{TiO}_2$ ;  $\text{Fe}_2\text{O}_3$  films from this figure , it is clear that  $n$  decrease with low concentration and increase with high concentration after doped that mean the density is decreased of this films.

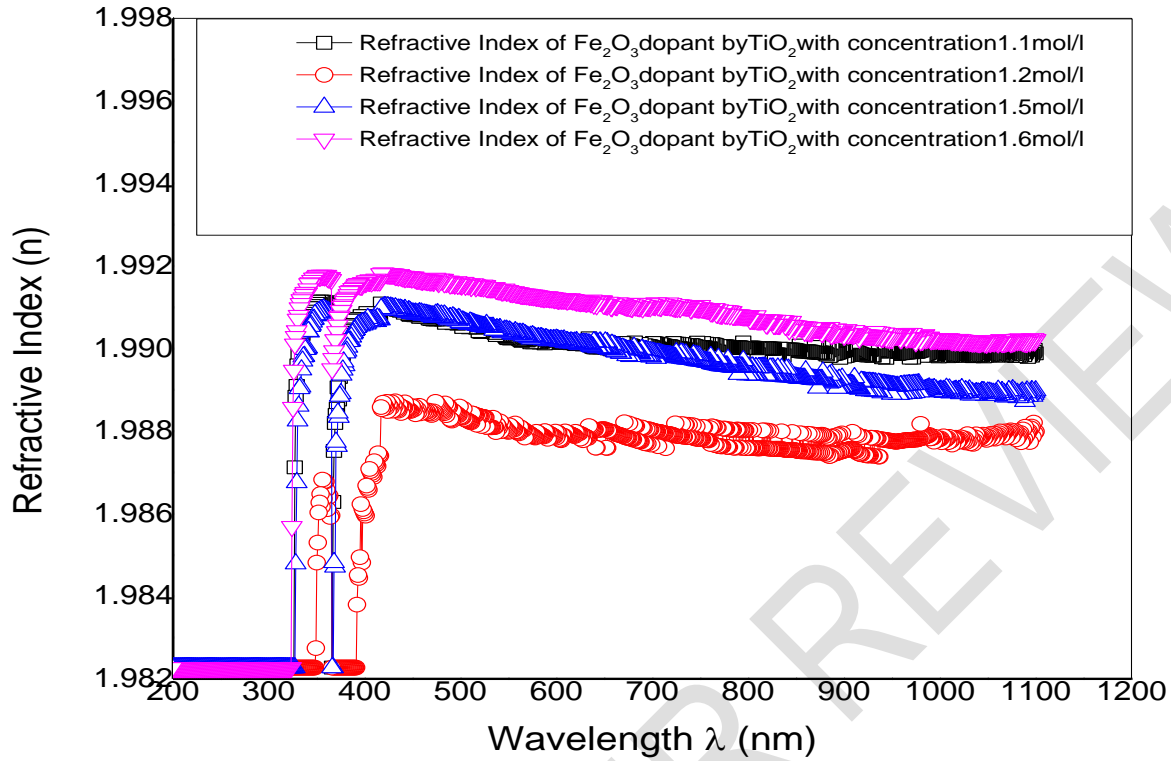


**Fig.12. Refractive index vs. wavelength plot of Fe<sub>2</sub>O<sub>3</sub> after doped TiO<sub>2</sub> thin films different at concentration (1.1, 1.2, 1.5 and 1.6mol/L)**

Fig (13) shows the extinction coefficient of TiO<sub>2</sub>:Fe<sub>2</sub>O<sub>3</sub> thin films before and after doped with different concentration (1.1, 1.2, 1.5 and 1.6) and in the range of (100 – 1200) nm. It can observe from this figure that the extinction coefficient, decrease sharply with the increase of wavelength for all prepared films and notice all the sample interference between them and this decrease start in all case from (700 until 200)nm. The extinction coefficient of the film was calculated approximately from the following relation: -

$$k = \frac{A}{C} \dots\dots\dots (5)$$

Where **k** the extinction coefficient, A is the absorbance and C is the concentration

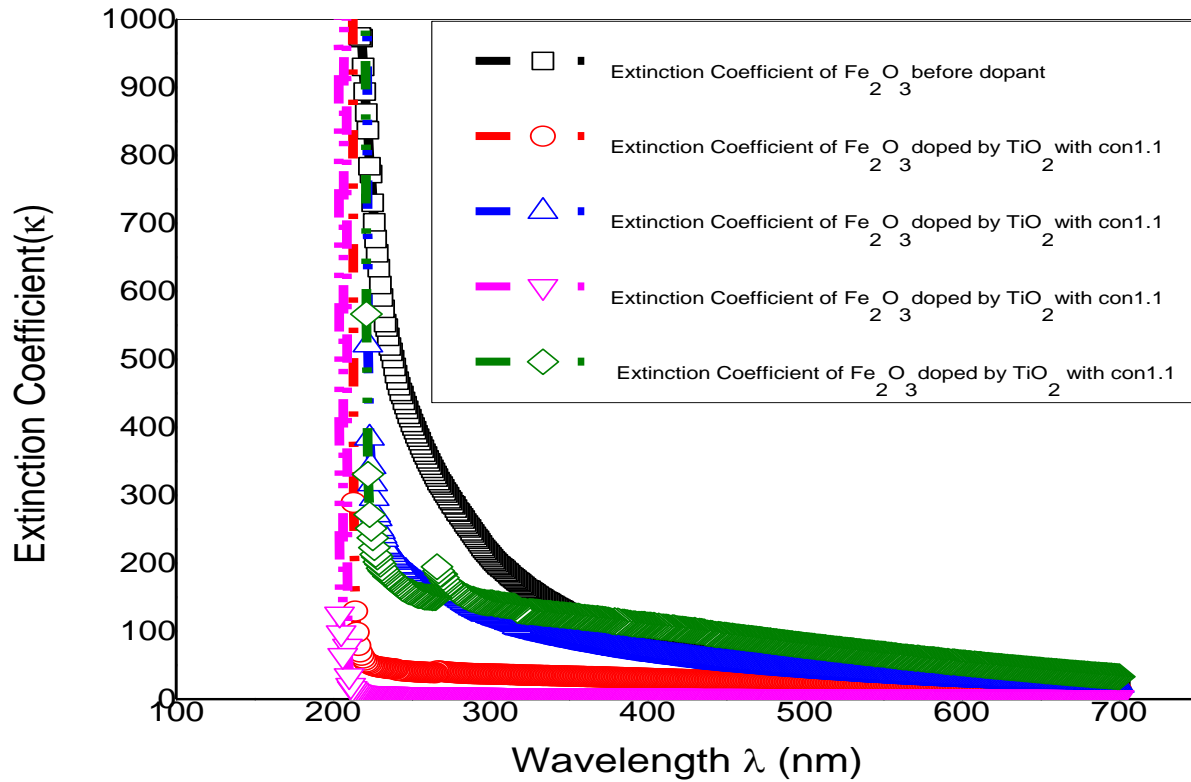


**Fig. (13).Extinction Coefficient vs. wavelength plot of Fe<sub>2</sub>O<sub>3</sub> before doped and after doped TiO<sub>2</sub> thin films at different concentration (1.1, 1.2, 1.5 and 1.6 mol/L)**

#### 4. Conclusion

This study is conducted to show the effect of TiO<sub>2</sub>:Fe<sub>2</sub>O<sub>3</sub> doped to increase the efficiency of thin film in a DSSC. Iron oxide with different concentration (1.1, 1.2, 1.5 and 1.6 mol/L) doped with titanium oxide; spray pyrolysis deposition method has been used to produce titanium oxide thin film. For the spraying technique, it will be altered to achieve film with better structure and porosity. The results obtained showed that doping of titanium oxide increase the efficiency of TiO<sub>2</sub> thin film in DSSC. It also proves that the fabrication of TiO<sub>2</sub> thin films by spray pyrolysis deposition method is successful.

#### 5. Recommendations:-

The major challenge in the fabrication and commercialization of DSSC is the low conversion efficiency and stability of the cell. The degradation of the cell based on dye sensitization, undesirable electrolyte properties and poor contact with the electrodes are the main causes of the poor performance of DSSC. To enhance the performance of the DSSC, several research directions are suggested: (i) improving the dye stability by finding the optimum parameters to slow the dye degradation; (ii) improving the dye structure to absorb more light at longer wavelengths, 780-2500 nm (the near infrared region, NIR); (iii) improving the morphology of semiconductors to attaining the best electronic conduction to reduce the dark current; (iv) using dye and electrolyte additives to enhance the cell performance; and (v) improving the mechanical contact between the two electrode. Thus, the choice of materials is very important in the fabrication and deployment of DSSCs because the conversion efficiency and stability of the cell do not depend on a single factor alone.

## Reference to a journal:

1. A Study on the Optimization of Dye-Sensitized Solar Cells Md Imran Khan University of South Florida.
2. Characterization of the Dye Sensitized Solar Cell A Major Qualifying Project Report Submitted to the Faculty of WORCESTER POLYTECHNIC INSTITUTE Project Code: MQPBD4JPD1.
3. Performance of dye-sensitized solar cell based on metal-deposited BiFeO<sub>3</sub> nanoparticles Submitted by Imanpreet Kaur Roll No: 301104007.
4. Reshak. A. H, Shahimin. M. M, Shaari. S, Johan N., Progress in Biophysics and Molecular Biology, 113 (2) (2013) 327-332.
5. Grant. C. D, Schwartzberg. A. M, Smestad. G. P, Kowalik. J, L. Tolbert. M. and Zhang. J. Z, Inorg Chem, 522 (1) (2002) 40-48.
6. Karuppuchamy. S, Nonomura. K, Yoshida. T, Sugiura. T. and Minoura. H, Solid State Ionics, 151 (1) (2002) 19-27.
7. Reshak. A. H, Shahimin. M. M, Juhari. N. and Vairavan. R, Curr. Appl. Phys., 13 (9) (2013) 1894-1898.
8. Kuzmych, O., Nonomura, K., Johansson, E.M.J., Nyberg, T., Hagfeldt, A., Skompska, M., Defect minimization and morphology optimization in TiO<sub>2</sub> nanotube thin films, grown on transparent conducting substrate, for dye synthesized solar cell application, Thin Solid Films 2012, 522, 71–78.
9. O'Regan. B, and. Grätzel. M, Nature 353 (1991) 737-740.
10. Chergui. Y, Nehaoua. N, Mekki. D. E, Solar Cells - Dye-Sensitized Devices, IntechOpen (2011) 49-64.
11. Khan, Md Imran, "A Study on the Optimization of Dye-Sensitized Solar Cells" Graduate Theses and Dissertations. <http://scholarcommons.usf.edu/etd/4519> (2013).
12. Robel, I., Subramanian, V., Kuno, M., Kamat, P. V. J. Am. Chem. Soc, 128, 2385 (2006).
13. Grätzel, M.. Photochem. Photobiol. C, 4, 145 (2003).
14. Chun, K.Y.; Park, B.W.; Sung, Y.M.; Kwak, D.J.; Hyun, Y.T.; Park, M.W. Thin Solid Films, 517 (14) 4196-4198 (2009).
15. Zhong. M, Jingying Shi, Wenhua Zhang, Hongxian Han, Can Li, Charge, J. Mater. Sci. Eng, B 176, 1115–1122 (2011).
16. Tennakone. K, Kumara. G, Kottegoda. I.R.M, Perera. V.P.S., Commun. Chem, 32, 15-16 (1999).
17. Keis. K, Magnusson. E, Lindstrom. H, Lindquist. S.E, Hagfeldt. A, Mater. Sol. Cells 73, 51-58 (2002).
18. Guo. P, Aegerter. M.A, Thin Solid Films, 351, 290-294 (1999).
19. Tan. B, Toman. E, Li. Y.G, Wu. Y.Y, J. Am. Chem. Soc., 129, 4162 (2007).
20. Serrano. E, G. Rus, Renew. Sustain. Energy, Rev. 13, 2373 (2009).
21. Na-Phattalung S, Smith MF, Kim K, Du MH, Wei SH, Zhang SB, Limpijumngong S., First-principles study of native defects in anatase TiO<sub>2</sub> Phys. Rev. B 2006; 73(12), 125205: 1-6.
22. Hao S, Wu J, Huang Y, Lin J., Natural dyes as photosensitizers for dye-sensitized solar cell. Sol. Energy 2006; 80: 209–14.
23. Giuseppe C., et al., International journal of molecular sciences, 11 (1) (2010) 254-267.
24. Law .M, Greene. L. E, Johnson .J. C, Saykally .R. and Yang. P, Nat Mater, 4 (6) (2005) 455-459.